PERGAMON

International Journal of Multiphase Flow 26 (2000) 1565–1582

International Journal of Multiphase Flow

www.elsevier.com/locate/ijmulflow

Studies of wispy-annular flow using transient pressure gradient and optical measurements

N.J. Hawkes[a], C.J. Lawrence[b], G.F. Hewitt[b,*]

[a]*Baker-Jardine Ltd, Parsons Green, London, UK*
[b]*Imperial College of Science, Technology and Medicine, London, UK*

Received 12 June 1999; received in revised form 4 October 1999

Abstract

Measurements of the characteristics of annular two-phase flow at high mass fluxes are reported which confirm the existence and demonstrate the behaviour of core structures (wisps) in such flows. Measurements were made of pressure gradient fluctuations and of optical obscuration. These demonstrated that the core structures had frequencies typically of the order of 5–8 Hz and that they travelled at velocities approaching those of the gas.

Keywords: Gas–liquid flow; Vertical tubes; Air–water flow; Optical measurements

1. Introduction

In gas–liquid flows in vertical tubes, the *annular flow* regime exists at qualities (i.e., vapour mass flow fraction) above a few percent and is the most important regime in most industrial applications. In these applications, the mass fluxes are often very high (typically 1000 kg/m^2 s or more in industrial boiler systems). As the liquid mass flux is increased in annular flow, the liquid flow in the film tends to reach a roughly constant value with all the additional liquid being entrained as droplets in the gas core. Liquid flow fractions in the core of 90% or more are typical.

When the core liquid mass flow rate is very high, there is a range of evidence which suggests that the flow behaviour becomes interestingly different. Firstly, there is evidence that large

* Corresponding author.

0301-9322/00/$ - see front matter
PII: S0301-9322(99)00104-4

structures (''wisps'') are formed in the gas core whose precise source and configuration is at present poorly understood. The behaviour of the pressure gradient in this region is also anomalous in that the pressure gradient may *decrease* with increasing gas velocity at a constant liquid flow rate. The region is also characterised by large fluctuations in the pressure gradient and by a strong decrease in droplet mass transfer coefficient with increasing droplet concentration.

To our knowledge, the first observation of the core structures in annular flow was that of Bennett et al. (1965) who coined the name ''wispy-annular flow'' for the region where such structures occurred. The structures are actually quite difficult to observe using ordinary visualisation techniques (such as high speed cine photography) since the wall film in this regime tends to be highly disturbed with considerable bubble entrainment within it. The structures can be observed using X-ray radiography and Fig. 1 shows an X-radiograph taken of a flow in this regime. The X-ray picture shows a typical core structure. Bennett et al. state that:

> ...the ''wispy-annular'' regime was characterised by the nature of the entrained phase. The phase appeared to flow in large agglomerates somewhat resembling ectoplasm.

Bennett et al. investigated flow patterns in a vertical tube with steam–water flow over a range of pressures. Both high speed cine photography and X-radiography was used and Fig. 2 shows the flow pattern map which resulted from the study.

The right-most line on this map represents the limit of ''dryout'' (or ''burnout'') in the 3.66 m long electrically heated tube which was used to generate the flows starting with subcooled water at the entrance of the tube. As will be seen, the wispy-annular flow regime occupies a significant region and dryout can occur in this region or in annular flow as shown.

Also in 1965 (and referring to the work by Bennett et al.), Baker (1965) used an X-ray fluoroscopy system to study flow patterns in Refrigerant-11 vapour–liquid flows. The experiments were carried out at the Argonne National Laboratory, USA; the fluoroscopy system is illustrated in Fig. 3. The experiments were carried out with liquid/vapour density ratios ranging from 21 to 58. For water, the range of saturation pressures to give equivalent

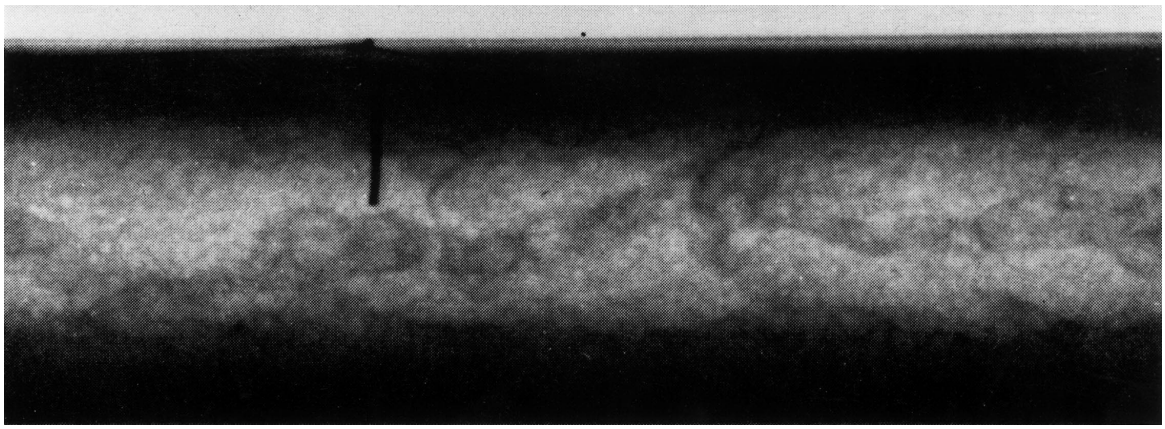

Fig. 1. X-ray flash radiograph of air–water flow in the wispy-annular regime (Bennett et al., 1965).

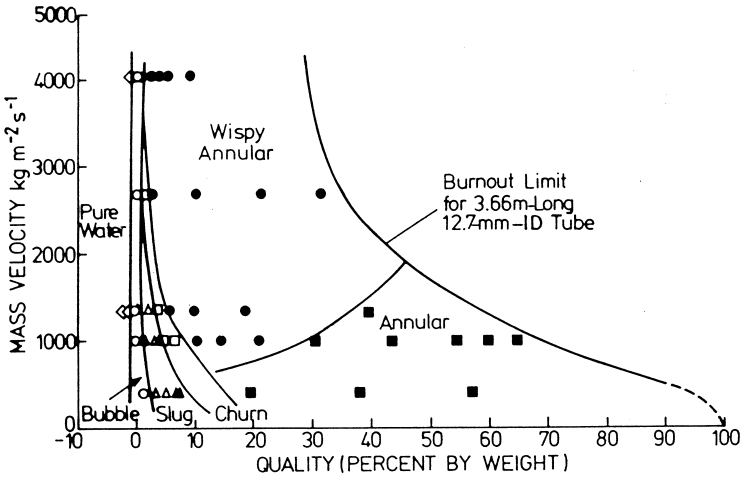

Fig. 2. Flow pattern map (including wispy-annular region) obtained by Bennett et al. (1965) for steam–water flow at 68.9 bar.

liquid/vapour density ratios would be 69 to 15 bar. Baker clearly observed the formation of wisps in the gas core and reported his observations as follows:

> The appearance of the usual liquid film on the walls of the conduit is supplemented by a different form of flow in the core. The vapour in the core appeared to transport agglomerates of liquid, which take on the appearance of billowy clouds of liquid rising in a similar manner to a wispy, turbulent stream of cigarette smoke.

Baker plotted the transition between annular, wispy-annular and churn flows for the various

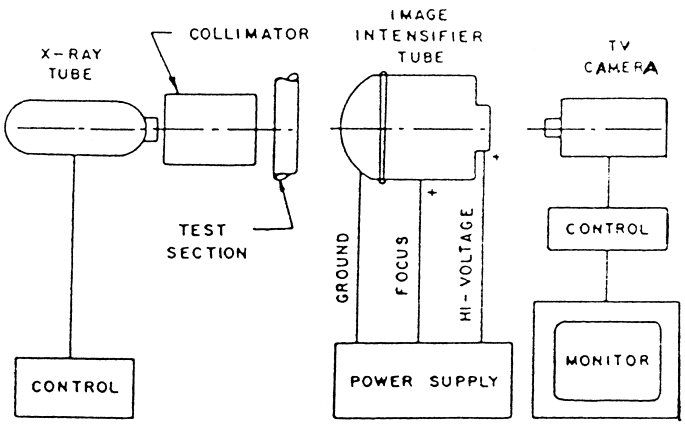

Fig. 3. Schematic diagram of the fluoroscope system used by Baker (1965).

pressure ratios and his results are shown in Fig. 4. Qualitatively, the results were similar to those obtained by Bennett et al. (1965).

Extending the observations of Bennett et al. (1965), Hewitt and Roberts (1969) were able to reconcile the data for air–water and steam–water flows by plotting the data in a map in terms of the superficial momentum fluxes (density multiplied by the square of the superficial velocity) for each phase and their resulting flow pattern map is shown in Fig. 5. This map has been found to fit a reasonably large range of fluids (including refrigerants) and is of particular interest in the high mass flux region. As the superficial gas momentum flux increases at high values of the liquid superficial momentum flux, there is a direct transition between a developing bubbly flow and the wispy-annular flow, with no intermediate slug or churn flow regions.

It is rather surprising that there has subsequently been a dearth of further observations of the regions of existence of wispy-annular flow and of the detailed characteristics of these flows. The probable explanation is that they are actually quite difficult to visualise; X-radiography or

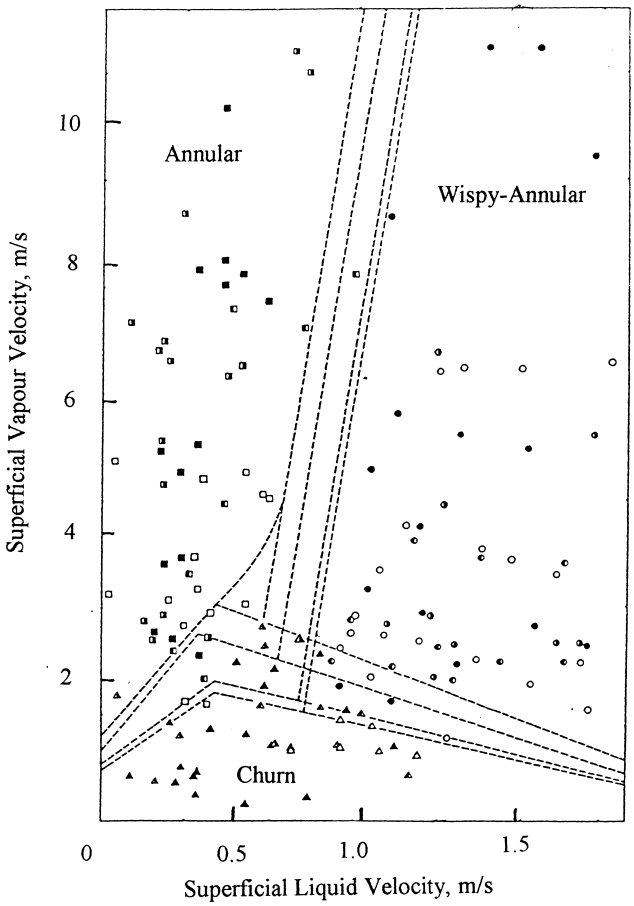

Fig. 4. Flow transition data obtained by Baker (1965) for Refrigerant-11 flows at various pressures.

equivalent techniques are needed to observe the structures and such techniques are expensive and difficult to apply.

Other manifestations of anomalous behaviour in annular flow at high mass fluxes include:

1. A rapid reduction of droplet mass transfer coefficient at high droplet concentrations (Bennett et al., 1967; Govan et al., 1988; Govan, 1990).
2. The existence of peaks in plots of pressure gradient as a function of gas mass flux at constant liquid–mass flux and pressure (Owen and Hewitt, 1987).

Hewitt (1997) argues that these phenomena are linked to the formation of the core structures characteristic of wispy-annular flow.

There has been surprisingly little investigation of the wispy-annular regime despite its evident industrial relevance. This perhaps reflects the fact that ordinary annular flow is in itself very complex, particularly in its interfacial structure and in the processes of droplet deposition and entrainment. Ordinary annular flow cannot yet be predicted with any degree of certainty, therefore, it is natural that investigators have steered clear of the additional complications associated with wispy-annular flow. The experiments described in this paper were carried out in an attempt to begin to rectify this situation and to provide new and more quantitative data on the growth of the interesting core structures.

Essentially, two experimental studies were performed, both using the LOTUS (Long Tube System) facility (formerly at the UKAEA's Harwell Laboratory and now at Imperial College). In the first study, measurements were made of fluctuating pressure drop; in the second study, an optical obscuration method was employed for evaluating and tracking the core structures. These two studies are presented in Sections 2 and 3, respectively. As will be seen, they provide new evidence of the existence and the behaviour of the core structures. More details of these studies (and of corroborating ones in other facilities) are given by Hawkes (1996).

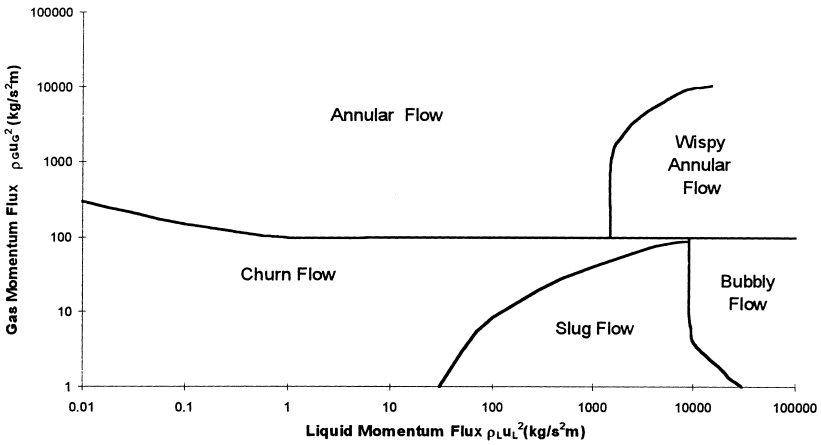

Fig. 5. Flow pattern map of Hewitt and Roberts (1969).

2. Measurements of pressure gradient

2.1. The LOTUS facility

LOTUS is the main experimental facility used in this study. A system flowsheet is given in Fig. 6. The facility spans four floors of the Pilot Plant Laboratory in the Department of Chemical Engineering and Chemical Technology at Imperial College, London.

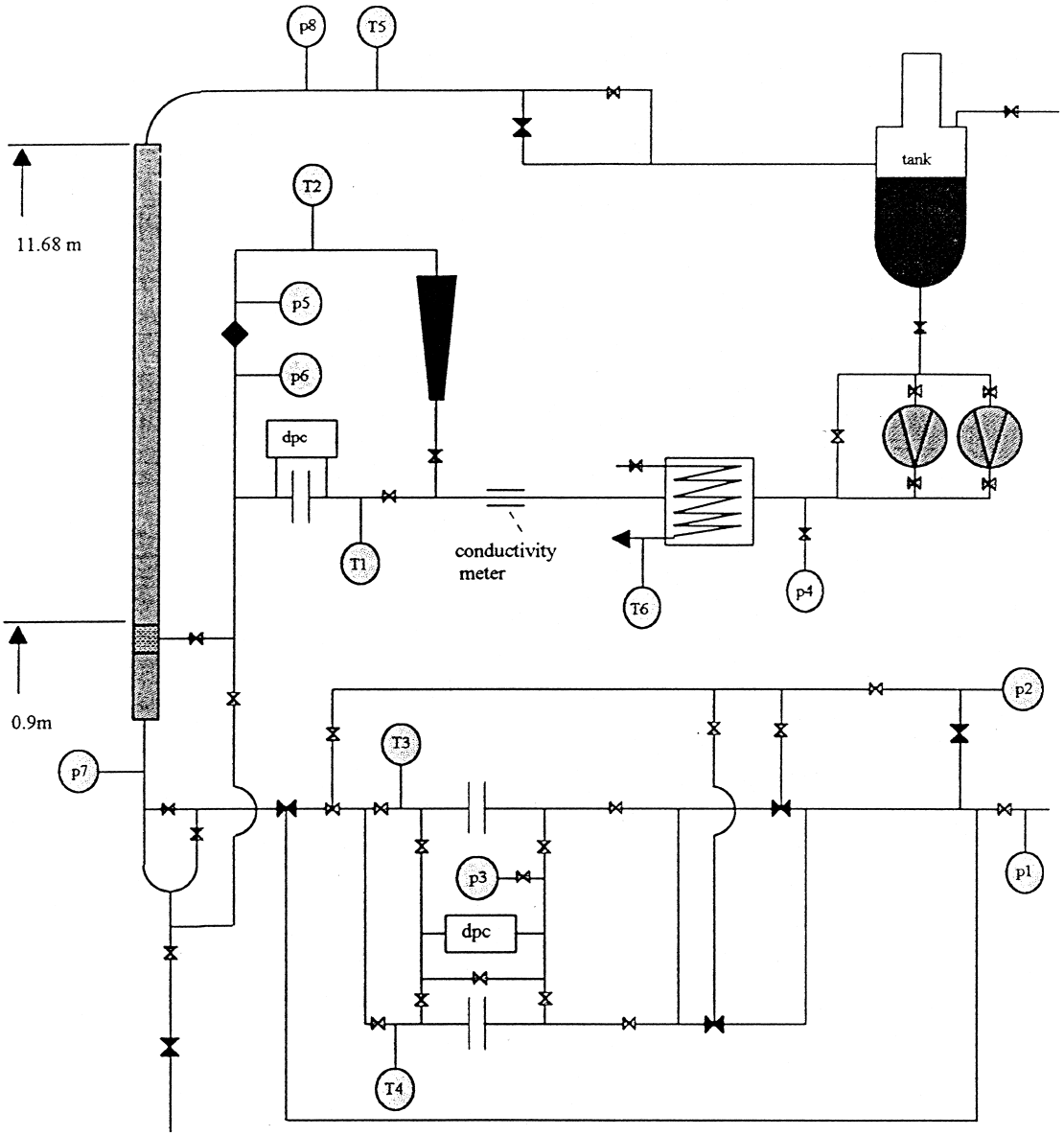

Fig. 6. Schematic diagram of the LOTUS facility.

LOTUS is a vertical two-phase air–water flow system that was originally built at the Harwell Laboratory of the UKAEA in the early 1960s. It was relocated to Imperial College in 1992. The relocation and alterations made to the facility are described in the thesis of Wolf (1995). It consists of a long vertical copper tube, originally of around 19 m active length at Harwell but now with a shorter active length of 10.8 m and internal diameter 31.8 mm (1.25 in.). The tube consists of sections of various lengths from 5 cm to around 180 cm in length, which are attached to a vertical fixed beam which is aligned very accurately. Air is fed to the bottom of the tube via a large radius U-bend and metered via a differential pressure transducer attached to an orifice plate. The College air supply is quite stable and has a maximum static pressure of 6.55 barg (95 psig). An additional control rod was attached to valve #41 on the second floor with a handle on the third floor (similar in design to the rod attached to the pump bypass valve also on the second floor), which allows control of the air flowrate without the use of the pneumatic valves. This is extremely useful when using high gas flowrates.

Water can be fed at two positions along the tube, one is 0.9 m above the air U-bend and the other around 5.4 m above the air U-bend. The latter allows for the study of developing flow. Water can be pumped through the system using either of two water pumps (a 1.5 kW single-stage pump and an 8 kW two-stage pump). The water is metered via rotameters. For the lower liquid flowrates, the water enters through a porous wall section of the same internal diameter as the tube, though for the larger flowrates this had to be removed as it produced too high a resistance, and limited the maximum liquid injection rate.

The liquid flow is returned to the main water tank via a throttling valve and separation cyclone. The air phase is vented to atmosphere.

2.2. Measurement of pressure gradient

Pressure gradient measurements were made using a high frequency differential pressure transducer which measured the variation with time of the pressure difference over a 0.83 m length. The pipes connecting the transducer to the tapping points were filled with water, any gas present being purged out with water to avoid compressibility effects in the lines. The transducer was set to zero before the test commenced (i.e. removing the offset due to the lines being filled with water, the test section being full of air during this process). The signal, from 0 to 10 V representing 0 to 350 mbar, was fed through an amplifier and analogue-to-digital converter card to a personal computer and 30 s runs were stored at 1000 Hz. Measurements were taken with the lower tapping at distances of 0, 3.10, 6.71 and 9.65 m from the liquid injector. Thirty-one sets of conditions were investigated at each distance, with the same gas and liquid flowrates being used as in the entrained fraction measurements.

The pressure drop between the pressure tappings was recorded continuously for 30 s. All the experiments were conducted at a fixed outlet pressure of 1.034 barg (15 psig). The signal was time averaged to give a mean value of pressure gradient and was also analysed using a proprietary spectral analysis code (DATS, see Wolf, 1995) to give the power spectrum of the fluctuations in pressure gradient.

2.3. Time averaged values of pressure gradient

The data obtained for time-averaged pressure gradient are illustrated in Fig. 7. The results are complex and demonstrate the complexity of the processes involved in annular and wispy-annular flow. There are several competing effects:

1. Because of liquid entrainment, the pressure gradient initially falls with distance; the thinner liquid film has a smoother surface and this gives rise to a lower pressure gradient. This is consistent with earlier observations (Gill and Hewitt, 1968; Wolf, 1995).
2. Due to the drop in pressure along the test section, the gas velocity increases and, ultimately, this leads to an increasing pressure gradient. However, previous studies (Brown, 1978) have shown that the flow approaches equilibrium *at the local pressure* (though this local pressure will continue to change with distance).
3. There are indications of the local inflections in the curves of pressure gradient versus gas mass flux at constant liquid mass flux which were observed by Owen and Hewitt (1987). However, in the present experiments, the range of gas mass flux was less than in the experiments of Owen and Hewitt and the peaks in the pressure gradient were not observed.

The combination of the above factors leads to a very complex variation of pressure gradient with length and with phase flowrates. Incidentally, this complexity is reflected in the difficulty of obtaining satisfactory relationships for pressure gradient in annular flow. For the present paper, however, it is sufficient to note the complex pattern, and particularly the effect of gas expansion.

2.4. Temporal fluctuations in pressure gradient

The signal from the differential pressure transducer was analysed using a proprietary signal analysis code (DATS, see Wolf, 1995) in order to obtain the probability density distribution for the signal and also to carry out spectral analysis. For the latter, a Fast Fourier Transform was performed leading to the determination of power spectral density as a function of frequency. For the higher liquid mass fluxes (notably 748 and 1029 kg/m^2 s) there were large fluctuations in the measured pressure drop. Probability density analysis showed that at the lower liquid fluxes i.e. annular flow, there was a very clearly defined peak in the pressure drop measurements while in 'wispy-annular' flow the probability function had a much greater standard deviation (spread). This could form the basis of flow regime recognition (Tutu, 1982, 1984). The relative sizes of the standard deviations of pressure gradients are shown in Fig. 8.

Sample graphs given in Fig. 9 illustrate the different forms of the spectral density functions. For the three flows considered we may observe the following phenomena:

1. For the upper set of curves (air flow rate 70 kg/m^2 s, water flow rate 358 kg/m^2 s), a peak appears at around 14 Hz with a second peak at around double this value. In normal annular flow (except at very low liquid flow rates), the most characteristic feature in the existence of *disturbance waves* which traverse the interface and are the source of liquid droplet entrainment etc. (Hall-Taylor et al., 1963). Visual observation using a high resolution video confirmed that this peak corresponded to normal disturbance waves and this flow is thus normal annular flow. The second peak is the first harmonic which

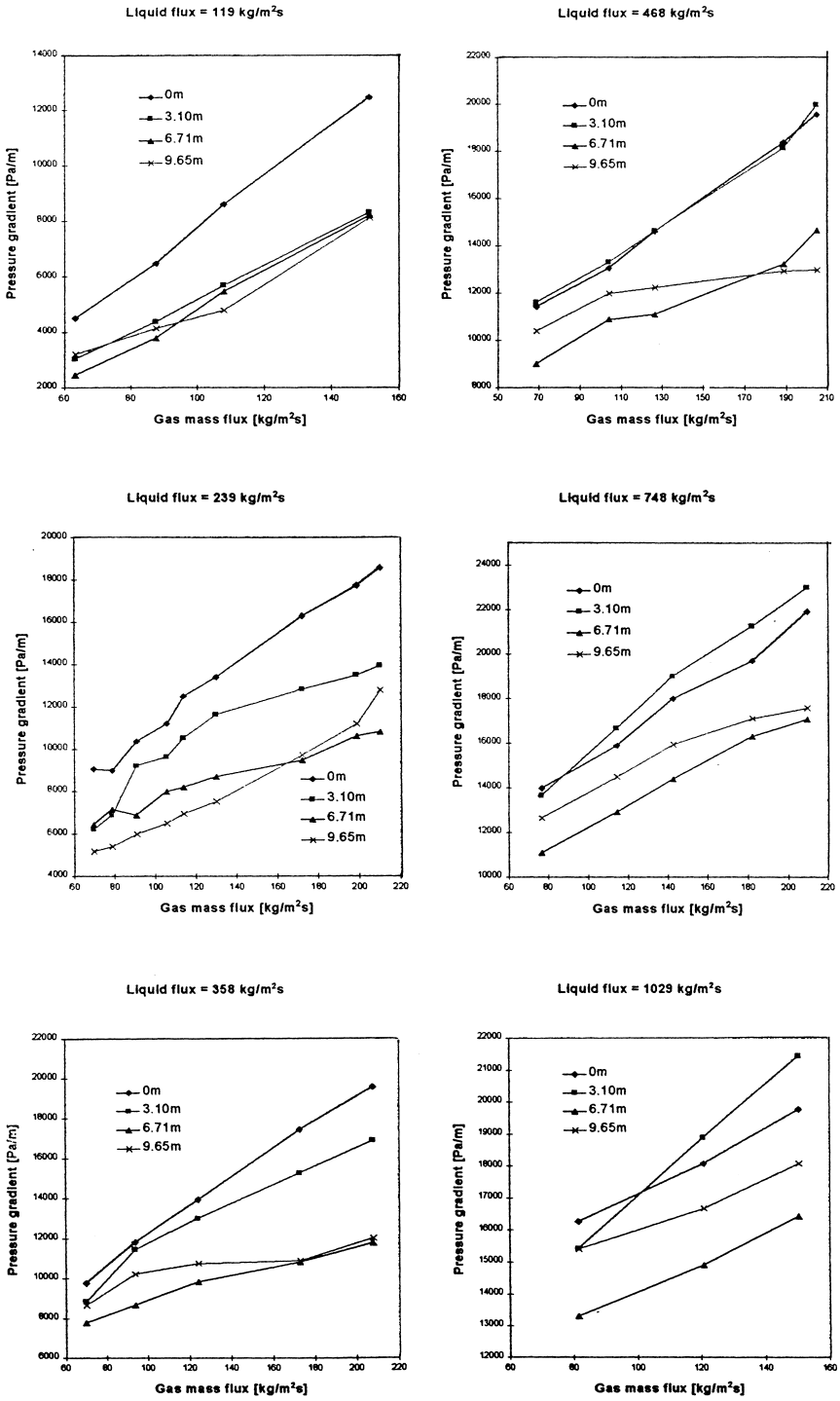

Fig. 7. Time averaged pressure gradient at different axial locations.

disappears gradually with length as the spectrum of the disturbance waves sharpens.

2. For the lower set of curves (air flow rate 82 kg/m^2 s and water flow rate 1029 kg/m^2 s), a peak appears at a much lower frequency, i.e. around 9 Hz initially but settling down to a value of around 5 Hz. A second peak can also be observed at around 14–16 Hz. When the flow is photographed using a video camera, periodic dark regions are observed where there is a dramatic reduction of light transmission through the flow. Visual observation showed that the lower frequency peak in the power spectral density of the pressure drop signal corresponded to the frequency of these dark zones and the upper frequency corresponded to the disturbance waves. This flow can be categorised as wispy-annular.
3. The middle set of power spectra (i.e. for an air flow of 114 kg/m^2 s and a water flow of 748 kg/m^2 s) show the initial formation of two peaks at around 18 and 5 Hz but the latter peak (corresponding to the dark zone) disappears towards the end of the pipe. Thus, this flow is on the boundary between annular and wispy-annular flow with the wisps being suppressed along the pipe, probably due to the increased gas velocity caused by the decrease in absolute pressure from the inlet to the outlet.

3. Measurements based on infra-red (IR) light transmission

In order to obtain more quantitative information about the behaviour of the core structures (wisps), an optical transmission method was used, not only to obtain frequency information

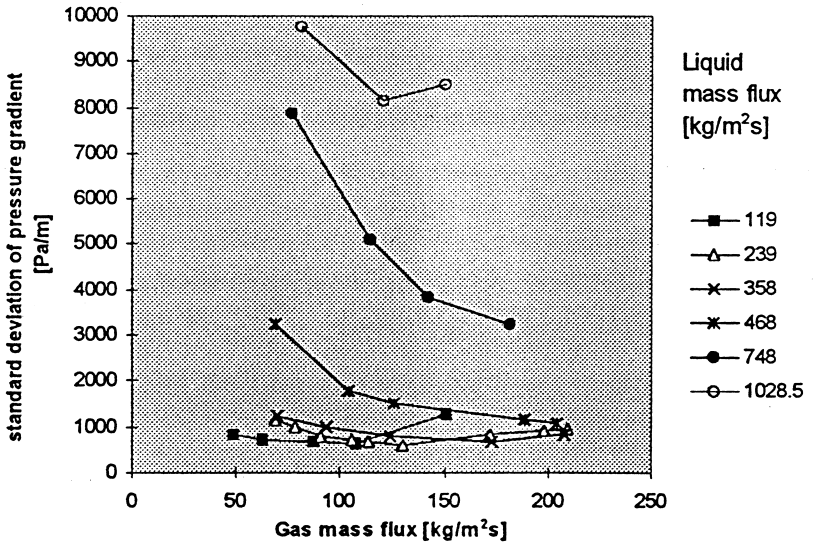

Fig. 8. Standard deviations of pressure gradient fluctuations.

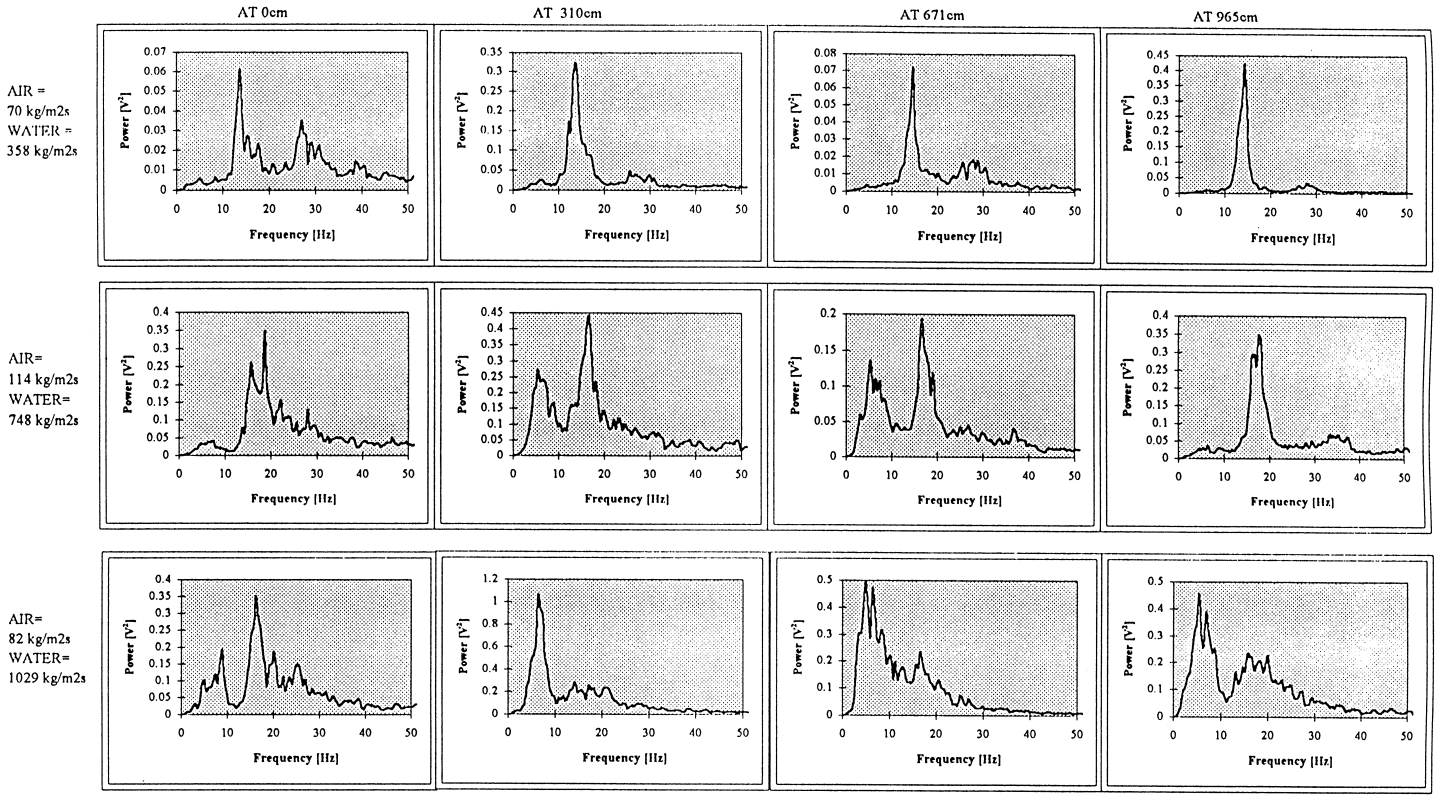

Fig. 9. Auto spectral density plots obtained from high frequency pressure gradient measurements.

supplementing the data obtained from the pressure gradient measurements but also to obtain information about the translational velocity of the core structures. The LOTUS facility (see Section 2.1) was again used and the outlet pressure was again controlled at 1.034 barg.

3.1. Infra-red light transmission system

This section describes the IR optical probe system which uses IR photo diodes and receivers mounted in light-tight housings on opposite sides of the tube respectively. IR was used rather than visible light since IR detectors are cheap and readily available. Light generated by the photodiode passes into the channel and any light not scattered in the flow enters the receiver on the opposite side of the tube. Two such units were constructed and mounted 10 cm apart at a distance of 10.4 and 10.5 m from the liquid injector. The power spectral density functions (described in Section 2.4) of pressure gradient measurements made at 1000 Hz had shown characteristic peaks in the annular and wispy-annular regime. There was a single peak at around 16 to 20 Hz for annular flow, with a second peak at around 4–7 Hz appearing as the liquid mass flux was increased and the wispy-annular flow regime was entered. From visual and low speed (50 frames/s) video observations, dark patches ('dark waves') were observed to travel along the tube; in these regions, light transmission through the mixture was minimal and it was this observation that led to the use of light scattering as a means of investigating and tracking these waves.

The new system was designed with two purposes in mind:

1. To investigate the features characteristic of annular and wispy-annular flow using a different measurement technique which, on the one hand, was more localised than the pressure gradient measurement and which, on the other hand, had a more rapid response than a gamma densitometer.[1]
2. To use cross-correlation of the signals from the two optical probes to obtain velocity measurements. These velocities should be of the 'disturbance waves' (16–20 Hz signal) and the 'wisps' in the core (5–8 Hz signal).

A schematic of the optical probe system is given in Fig. 10.

All the data were taken at axial distances of 10.4 and 10.5 m from the liquid inlet. The data from the IR receivers was collected on a personal computer (PC) at both 1000 and 7143 Hz. The maximum frequency of 7143 Hz was limited by the processing speed of the data collection computer. A maximum of 32,000 points of data could be collected in any one continuous run. Splitting this across the two channels that needed to be sampled simultaneously, this gave sample times of 16.0 and 2.24 s, respectively. Data were obtained for two conditions, namely those for developed annular/wispy-annular flow and those where the liquid film was removed immediately upstream of the optical probes. In this way, scattering events in the core of the flow (wisps or dark waves) could be discriminated from those associated with the liquid film (e.g. disturbance waves).

[1] A low power gamma densitometer was used in these studies but was only really suitable for obtaining time averaged liquid holdup (Hawkes, 1996).

These data samples were analysed using statistical analysis. The following analyses were done:

1. The signal was analysed via Fast Fourier Transforms to produce Auto Spectral Density plots showing any fundamental frequencies present in the signals.
2. The signals from the two sets of probes (separated by 0.1 m) were cross-correlated in order to determine the velocity of the scattering regions.
3. The velocities obtained from cross-correlation could then be used to calculate the slip ratio of liquid droplets/'wisps' in the gas core. This required knowledge of the film thickness and entrained fractions of liquid. The latter was previously measured at the gas and liquid flowrates of interest. The film thickness was calculated from the known film flowrate and pressure gradients using the 'triangular relationship' (see Hawkes, 1996).

3.2. Results using IR optical probes

A sample time trace received from the probes is shown in Fig. 11, the disturbance waves are clearly shown as 'troughs' in the signal.

The spectral analysis of the signals sampled at 7143 Hz led to the results with very coarse frequency resolution in the area of interest (from 0 to 50 Hz), with a 3.5 Hz increment being

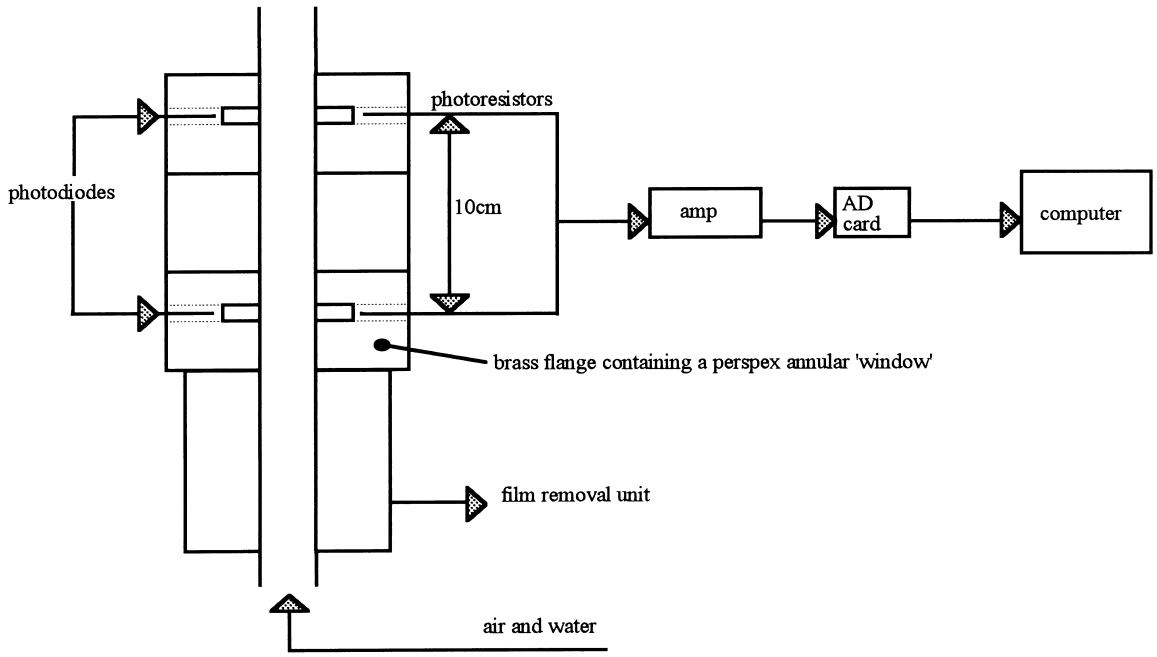

Fig. 10. Schematic of optical probe system.

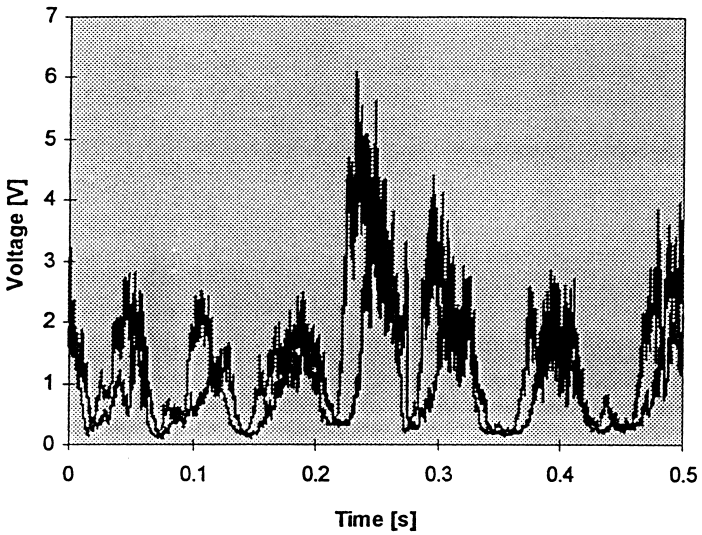

Fig. 11. Twin opitcal probe trace with the annular film present (air = 82 kg/m^2 s; water = 1029 kg/m^2 s).

the smallest increment that the specific Fourier analysis system used could produce. The 1000 Hz tests gave a frequency interval of 0.49 Hz. The spectra obtained at the latter frequency are typified by those shown in Fig. 13. Without removal of the film, two peaks in the power were observed for the example shown in Fig. 12, the peaks corresponded to around 15 and 6 Hz. It

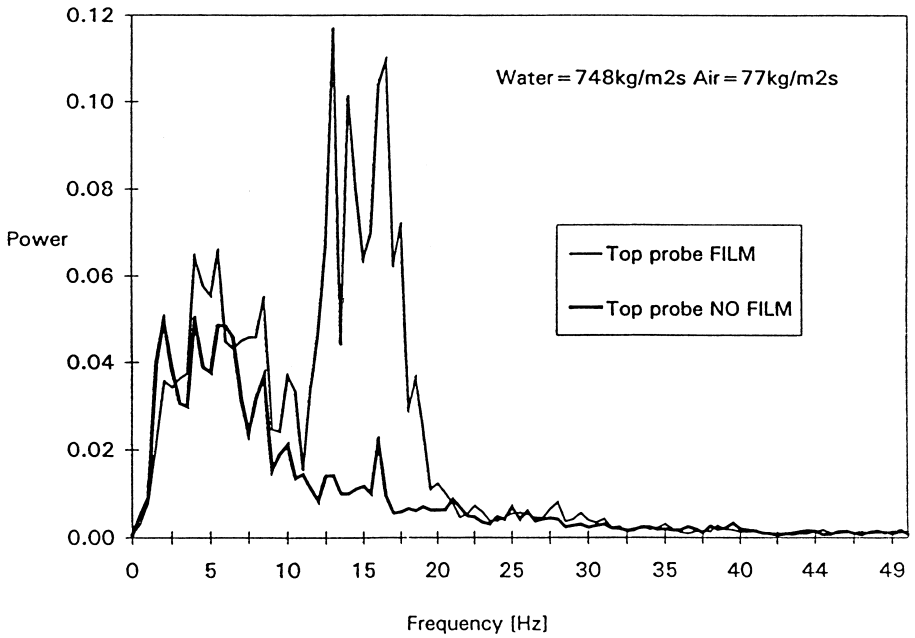

Fig. 12. Power spectral density plot from optical probe for wispy annular flow with and without film removal.

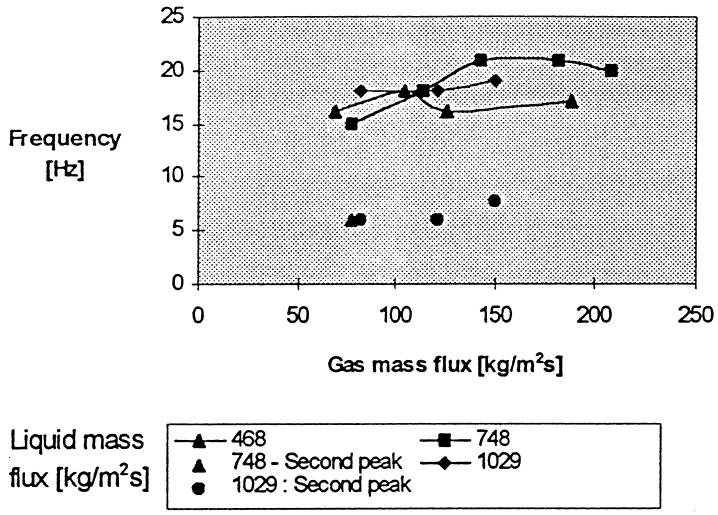

Fig. 13. Frequency of peaks in the spectrums of traces obtained with the optical probes.

is suggested that these peaks correspond to the disturbance waves and the core structures (wisps), respectively. This view is confirmed since, when the liquid film is extracted upstream of the optical probe system, the higher frequency peak disappears but the lower frequency peak characteristic of the core structures remains. These results are in good agreement with those obtained from the pressure drop spectra (see Section 3.1)

Fig. 13 shows the results obtained for peak frequency for the various experiments. In all tests, the 15–20 Hz peak (corresponding to disturbance waves) appeared. Only at the higher

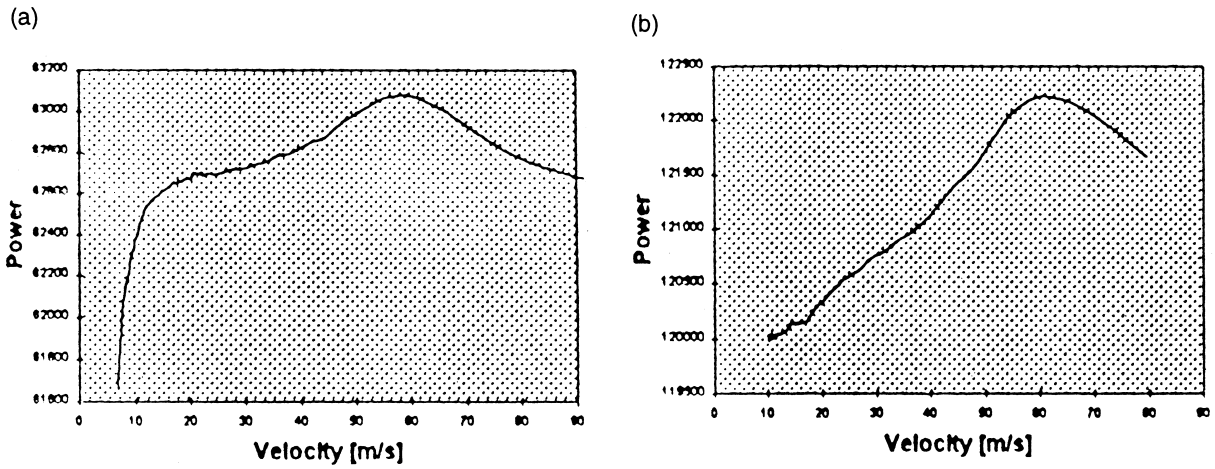

Fig. 14. Velocity cross spectra obtained from the outputs of the optical probes: (a) before film remover; (b) after film remover (air mass flux, 182 kg/m^2 s, liquid mass flux, 748 kg/m^2 s).

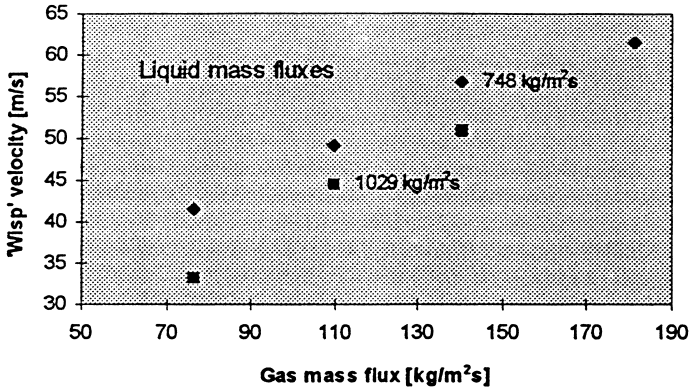

Fig. 15. Mean velocity of 'wisps' from cross correlation of optical probe data.

mass fluxes did the second peak at 5–8 Hz appear corresponding to the appearance of the core structures characteristic of wispy-annular flow.

The outputs from the optical probes could also be cross correlated to give the velocity of motion of the respective structures (disturbance waves and core structures or wisps). The cross correlation could be carried out with and without the liquid film removed upstream of the probes. Typical results are shown in Fig. 14. With the liquid film still present there is a broad band of signals at lower velocities (characteristic of the interfacial wave structures, including disturbance waves).

The disturbance waves have velocities of typically 10–20 m/s. A peak also occurs at around 60 m/s and this peak persists even when the liquid film is removed. Therefore, it is suggested that the peak represents the characteristic velocity of the core structures (wisps). These velocity measurements were confirmed by the analysis of high speed videos (2000 frames/s), tracing individual disturbance waves and "dark zones".

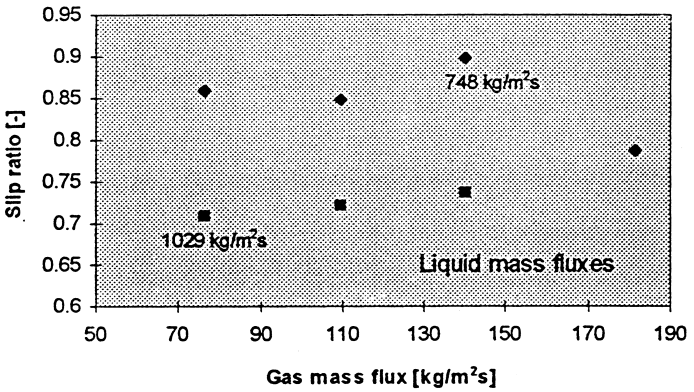

Fig. 16. Slip ratio of wisps (wisp velocity/mean gas velocity).

Figs. 15 and 16 show the results for wisp velocity and slip ratios (i.e. ratio of wisp velocity to mean gas velocity in the core). These results show the wisps are moving at velocities approaching that of the gas, the slip ratio decreasing with increasing liquid mass flux. This latter effect may be the result of agglomeration of liquid in the core structures leading to lower mean velocities of these structures.

4. Conclusion

The results presented here provide new evidence on the behaviour of core structures (wisps) in annular flow at high mass fluxes. The wisps appear to have frequencies of the order of 5–8 Hz and to travel at velocities approaching that of the core.

The exact source of these core structures has yet to be established but one explanation is that they are a manifestation of instability of the highly concentrated gas–droplet mixture in the core to small perturbations in concentration. This is analogous to the formation of void waves in bubbly flow and the formation of concentration waves in fast fluidisation. This concept is pursued further by Hawkes et al. (1999).

The optical probe technique used here is not capable of indicating the concentration of the liquid in the core structures. Measurements were made using a gamma densitometer (Hawkes, 1996) which indicated that the concentration was likely to be rather small (of the order of a few percent by volume) but the resolution was inadequate to obtain an accurate figure. Further studies are now underway with a much more powerful densitometer.

Acknowledgements

The authors wish to acknowledge with thanks the support given to this project by the UK Engineering and Physical Sciences Research Council (EPSRC).

References

Baker, J.L.L., 1965. Flow regime transitions at elevated pressures in vertical two-phase flow. Argonne National Laboratory Report No. ANL-7093, September 1965.

Bennett, A.W., Hewitt, G.F., Kearsey, H.A., Keeys, R.K.F., Lacey, P.N.C., 1965. Flow visualisation studies of boiling at high pressure. Proc. Inst. Mech. Eng. 180 (Part 3C), 1–11.

Bennett, A.W., Hewitt, G.F., Kearsey, H.A., Keeys, R.K.F., Pulling, D.J., 1967. Studies of burnout in boiling heat transfer. Trans. Inst. Chem. Eng. 45, 319–333.

Brown, D.J., 1978. Disequilibrium in annular flow. D. Phil. Thesis, University of Oxford.

Gill, L.E., Hewitt, G.F., 1968. Sampling probe studies of the gas core in annular two-phase flow. Part III: Distribution of velocity and droplet flowrate after injection through an axial jet. Chem. Eng. Sci. 23, 677–686.

Govan, A.H., 1990. Modelling of vertical annular and dispersed two-phase flows. Ph.D. Thesis, University of London.

Govan, A.H., Hewitt, G.F., Owen, D.G., Bott, T.R., 1998. An improved CHF modelling code. Proc. Second Heat Transfer Conference, Glasgow, September 14–16, 1988, Mechanical Engineering Publications (MEP), London, vol. 1, pp. 33–48.

Hall-Taylor, N.S., Hewitt, G.F., Lacey, P.N.C., 1963. The motion and frequency of large disturbance waves in annular two-phase flow of air–water mixtures. Chem. Eng. Sci. 16, 537–552.

Hawkes, N.J., 1996. Wispy-annular flow. Ph.D. Thesis, University of London.

Hawkes, N.J., Lawrence, C.J., Hewitt, G.F., 1999. Prediction of the transition from annular to wispy-annular flow using linear stability analysis of the gas-droplet core. Chem. Eng. Sci. (submitted for publication).

Hewitt, G.F., 1997. Wisps in the pipe: annular flow at high mass fluxes. Proc. Fourth World Conference on Experimental Heat Transfer, Fluid Mechanics and Thermodynamics, Brussels, June 2–6, 1997, vol. 1, pp. 3–14.

Hewitt, G.F., Roberts, D.N., 1969. Studies of two-phase flow patterns by simultaneous X-ray and flash photography. UKAEA Resport No. AERE-M2159, February 1969.

Owen, D.G., Hewitt, G.F., 1987. An improved annular two-phase flow model. Proc. Third Int. Conf. on Multiphase Flow, The Hague, the Netherlands, paper C1.

Tutu, N.K., 1982. Pressure fluctuations and flow pattern recognition in vertical two-phase gas liquid flows. Int. J. Multiphase Flow 8, 443–447.

Tutu, N.K., 1984. Pressure drop fluctuations and bubble slug transition in vertical two-phase air-water flow. Int. J. Multiphase Flow 10, 211–216.

Wolf, A., 1995. Film structure of vertical annular flow. Ph.D. Thesis, University of London.